Published in final edited form as:
ACS Chem Biol. 2012 September 21; 7(9): 1596–1602. doi:10.1021/cb300130k.

Revisiting the Role of Glycosylation in the Structure of Human IgG Fc

M. Jack Borrok[a], **Sang Taek Jung**[a], **Tae Hyun Kang**[b], **Arthur F. Monzingo**[c], and **George Georgiou**[a,b,c,d,*]

[a]Department of Chemical Engineering, University of Texas, Austin, TX 78712, USA

[b]Department of Biomedical Engineering, University of Texas, Austin, TX 78712, USA

[c]Institute for Cellular and Molecular Biology, University of Texas, Austin, TX 78712, USA

[d]Section of Molecular Genetics and Microbiology, University of Texas, Austin, TX 78712, USA

Abstract

Binding of the Fc domain of Immunoglobulin G (IgG) to Fcγ receptors on leukocytes can initiate a series of signaling events resulting in antibody-dependent cell-mediated cytotoxicity (ADCC) and other important immune responses. Fc domains lacking glycosylation at N297 have greatly diminished Fcγ receptor binding and lack the ability to initiate a robust ADCC response. Earlier structural studies of Fc domains with either full length or truncated N297 glycans led to the proposal that these glycans can stabilize an "open" Fc conformation recognized by Fcγ receptors. We determined the structure of an *E. coli* expressed, aglycosylated human Fc domain at 3.1 Å resolution and observed significant disorder in the C′E loop, a region critical for Fcγ receptor binding, as well as a decrease in distance between the CH2 domains relative to glycosylated Fc structures. However, comparison of the aglycosylated human Fc structure with enzymatically deglycosylated Fc structures revealed large differences in the relative orientations and distances between C_H2 domains. To provide a better appreciation of the physiologically relevant conformation of the Fc domain in solution, we determined Radii of Gyration (R_g) by small angle X-ray scattering (SAXS) and found that the aglycosylated Fc displays a larger R_g than glycosylated Fc, suggesting a more open C_H2 orientation under these conditions. Moreover, the R_g of aglycosylated Fc was reduced by mutations at the C_H2-C_H3 interface (E382V/M428I), which confer highly selective binding to FcγRI and novel biological activities.

Keywords

Immunoglobulin G; Fc; aglycosylated; Antibody-dependent cell-mediated cytotoxicity; X-ray crystal structure; Small angle X-ray Scattering

The Fragment crystallizable (Fc) portion of antibodies provides a link between both the innate and adaptive immune systems as well as between humoral and cellular immunity. Antibodies, whether generated by our own immune systems or administered therapeutically,

*For correspondence: gg@che.utexas.edu.

The authors declare not conflict of interest

Author contributions:
MJB and GG designed research; MJB, THK, and STJ, AFM performed research and generated reagents; MJB and GG analyzed data; MJB and GG wrote the paper.

Accession Codes
The coordinates of the aglycosylated human IgG1 Fc have been deposited in the Protein Data Bank with the accession number 3S7G.

interact with Fc gamma receptors (FcγRs) and complement components (such as C1q) to clear pathogens or to destroy aberrant cells such as tumors.(1, 2) Antibodies of the immunoglobulin G (IgG) subclass are composed of two identical Fragment antigen binding (Fab) domains containing variable regions which bind to antigen and a single Fc domain which mediates effector functions such as antibody-dependent cell-mediated cytotoxicity (ADCC) and antibody-dependent cell-mediated phagocytosis (ADCP) via FcγRs and complement dependent cytotoxicity (CDC) via C1q.(3)

The horseshoe-shaped, homodimeric Fc domain consists of two C_H2 domains at the N-terminus and two interacting C_H3 domains at its C-terminus. Although the two C_H2 domains do not directly interact, the N-linked glycosylation at N297 bridges the gap between the two domains while shielding the hydrophobic inner surface of C_H2 from solvent. The N297 glycan consists of a core heptasaccharide (GlcNAc4Man3) chain that can be appended by the addition of fucose at the initial GlcNAc residue or galactose residues at terminal GlcNAc.(4) Additionally, sialic acid residues can also be added to terminal galactose residues. The complete removal of the glycan at N297 greatly reduces binding to effector FcγRs expressed by B cells, natural killer (NK) cells, granulocytes, and monocytes as well as to the complement protein C1q, thus significantly diminishing ADCC and CDC.(5–7) While extensive glycan truncations have been shown to be deleterious to the ability of the Fc domain to interact with FcγRs, certain changes in the glycan composition can actually promote favorable effector interactions. Indeed, efforts have focused on the engineering of monoclonal antibodies with glycans optimized for various effector functions.(8, 9) For example, defucosylation of the N297 glycan has been reported to enhanced binding of FcγRIIIa and increase NK mediated ADCC by >50 fold.(10–13)

The X-ray structures of four different Fc domains with distinct glycan truncations suggested that shortening of the N297 glycan results in progressively more “closed” conformations, bringing the C_H2 domains in closer proximity compared to fully glycosylated, “open” Fc conformer.(14) These observations led to the prevailing model that the “open” conformation of glycosylated Fc is critical for physiologically relevant binding to the effector FcγRs. Additionally, the crystal structure of glycan truncation variants revealed minor conformational changes within the C′E loops of the Fc domain.(14) As no aglycosylated human Fc structure has yet been described, the exact structural reasons responsible for loss of effector binding affinity in aglycosylated antibodies are unknown. However, a recent structure of an enzymatically deglycosylated murine Fc exhibited a “super-closed” state with the C_H2 domains collapsing toward one another.(15) The observed Fc conformation was consistent with the model that disruption of the open conformation is responsible for the abrogation of FcγR binding and lack of ADCC displayed by aglycosylated Fc domains. It should be noted that unlike the large movements in C_H2 observed when the glycans are truncated or removed, the C_H3 domain shows essentially no structural perturbation.

Technical advances in recent years led to the high yield preparative expression of aglycosylated antibodies in bacteria and methods for the isolation of full length IgGs from combinatorial libraries expressed in *E. coli*.(16–18) Several antibodies lacking glycosylation are now under advanced clinical evaluation.(19) For some therapeutic applications the lack of ADCC/CDC exhibited by aglycosylated antibodies is a preferred property, however, in many cases (such as with some anti-tumor antibodies) ADCC or CDC is desired. Aglycosylated antibodies with restored or tailored ADCC properties are currently under investigation. Recently, the screening of large combinatorial libraries has led to the isolation of aglycosylated Fc variants that bind selectively only to FcγRI(20) or alternatively to the both the activating FcγRIIa and the inhibitory FcγRIIb receptors(21) with high affinity. In particular, the FcγRI selective aglycosylated Fc5 variant, containing two mutations E382V/

M428I, was shown to uniquely induce cytotoxicity of target cells with monocyte-derived dendritic cells as effectors, a phenotype not conferred by glycosylated IgG.(20)

The mutations in Fc5 are near the C_H2-C_H3 interface and distal to the FcγRI binding epitope.(22, 23) This finding raises several questions specifically about the nature of the Fc5:FcγRI interaction and more generally about the importance of the "open" conformation of Fc domains. To address these issues we first solved the structure of a human aglycosylated Fc. Analysis of this and other crystallographic information suggests that the proposed "closed" conformations of aglycosylated Fcs observed in crystals may not be the physiologically relevant form. SAXS analysis further revealed that aglycosylated Fc actually has a larger Radius of gyration (R_g) than glycosylated Fc in solution. The aglycosylated Fc5 displays an intermediate R_g in solution indicating that the degree of "openness" of the aglycosylated Fc can be altered by mutations selected to restore FcγRI binding.

Results and Discussion

The Structure of Aglycosylated Human IgG1 Fc

The structure of human IgG1 Fc purified from *E. coli* and therefore lacking glycosylation was solved at 3.1 Å resolution. The crystal was in the P1 space group with two Fc dimers (composed of polypeptides A,B and C,D respectively) in the asymmetric unit (Figure 1). The two Fc dimers also interface at the C_H2- C_H3 elbow of chains A and C. Phasing by molecular replacement and refinement led to a final model with an R- factor of 26.2% (Rfree = 32.3%) (Table 1). To reduce structural bias the C_H2 and C_H3 domains were treated as separate entities during molecular replacement and refinement, with residues bridging the C_H2-C_H3 domains removed from non-crystallographic symmetry restraints.

The four polypeptides (A–D) are composed of residues G236-L443, G236-S442, G237-S444, P238-S444 respectively with electron density for amino acids 221–235 (composing the IgG hinge) and 445–447 missing in all chains. Hinge residues in all Fc structures to date have been unobservable in electron density maps presumably due to their high flexibility. (14) Electron density maps were generally well defined and provided unambiguous interpretation of most coordinates, with the exception of small regions of the C′E, BC, and FG loops in the upper C_H2 domain of chains B and D. The high temperature factors and sparse electron density in the upper C_H2 loops of B and D may be due to tight packing interactions with symmetry related Fcs within the crystal lattice.

C′E loop orientation

The orientation of the C′E loop (which harbors the Fc glycosylation site at N297) is critical for effector FcγR binding.(14, 24) Alteration in the glycan composition(14, 25) have been reported to cause perturbations in this loop that drastically reduce effector FcγR binding. (26, 27) The C_H2 domain of Chain A was compared with the C_H2 domain of a recently solved fully glycosylated Fc (PDB ID: 3AVE)(25, 28) revealing minor backbone deviation from the glycosylated structure in the C′E loop starting at P291 to approximately T299 (Figure 2a). The most pronounced difference are at Y296 and S298 (Figure 2a). Electron density for most of the Y296 and Q295 side chains was absent at 2σ density (2Fo-Fc). Comparison of the Y296 orientation of our structure with an aglycosylated human C_H2 domain alone(29) and with an enzymatically deglycosylated Fc structure (PDB ID: 3DNK) revealed different Y296 side chain orientations relative to each other and relative to glycosylated Fc structures (Figure 2b). The dramatic variability in Y296 is notable in light of the importance of this residue in FcγRIIIa and FcγRIIa binding.(30) Additionally, The human aglycosylated Fc structure displays high crystallographic temperature factors (*B*-factors) for the C′E loop, relative to the rest of the structure (Figure 1). Indeed, a more

dynamic/disordered C′E loop has been proposed to be among the reasons for the lack of effector Fcγ R binding in the absence of glycosylation.(14)

Comparison with other Fc structures

Superposition of the aglycosylated Fc A,B dimer with the human glycosylated Fc fragment 3AVE(25, 28) revealed that the former adopted a more closed orientation (C_H2 domains in closer proximity, Figure 3a). Distances between P329 (P332 in murine Fcs) in the upper C_H2 domains had been used previously to compare the relative "openness" of the C_H2 in Fc. (14, 32) With P329 distances of 18.9 Å and 19.6 Å for the A,B and C,D dimers, the aglycosylated structure is significantly more closed when compared with P329 distances of fully glycosylated Fc domains (Table 2).

A further comparison with a recent structure of deglycosylated Fc (obtained by expression in mammalian cells followed by enzymatic deglycosylation) revealed a much more complex picture (Figure 3b, Table 2). Whereas the murine deglycosylated Fc (PDB ID: 3HKF) was reported to adopt a "super closed" state with the $C_\gamma 2$ domains in very close proximity to one another (13.5 Å closer than in the glycosylated Fc 3AVE)(15), in a human deglycosylated Fc (PDB ID: 3DNK) the C_H2 domains assume a more open structure and are farther apart relative to many glycosylated Fc domains (Table 2). The Pro329 distance in that structure is in fact 9 Å greater compared to *E. coli* purified, aglycosylated Fc A,B dimer. It should be noted that the human deglycosylated Fc differs from the human aglycosylated Fc reported here by only 3 conservative amino acid changes, one of which, N297D, is due to the action of the deglycosylase PNGase F.

Small angle X-ray Scattering

The fairly dramatic difference in C_H2 domain proximity in the three Fc structures devoid of glycan may be due to artifacts induced by crystal packing effects. Indeed, high salt conditions during crystallization have been observed to alter Fc orientation in the crystal state.(14) To gain a better insight into the conformation of the Fc domain in solution we employed small angle X-ray scattering (SAXS). SAXS allows for accurate and precise measurement of a protein's radius of gyration (R_g), and has been used previously to differentiate between open or closed conformations in solution for numerous proteins.(33–35) In addition to glycosylated Fc and *E. coli* expressed aglycosylated Fc we also analyze the shape parameters of the aglycosylated Fc5 mutant (E382V/M428I) which confers selective binding to FcγRI and mediates dendritic cell activation and ADCC.(20)

Scattering curves of serially diluted Fc domains were extrapolated to zero concentration to account for concentration effects (Figure 4a). All three proteins exhibited Kratsky plots typical of well folded, non-aggregated samples (data not shown). As expected, scattering curves were quite similar with minor differences between the three samples visible in the higher resolution regions ($s < 0.15$, Figure 4a). Radii of gyration (R_g) were determined from zero concentration extrapolations of both short (0.5s) and long (5s) exposure data from the slope of Guinier plots.(36) Small but significant difference in R_g values of glycosylated Fc, aglycosylated Fc and the aglycosylated Fc5 mutant were observed (Table 3). Notably, the glycosylated Fc displayed an R_g of 27.4 ± 0.1 Å compared to an R_g of 28.3 ± 0.1 Å for aglycosylated Fc. This finding suggests that in solution the absence of glycosylation induces a more open conformation and not the "closed" form suggested by most of the crystallographic data, including ours.(14, 15) Interestingly, the R_g of aglycosylated Fc5 (27.9 ± 0.1 Å) was intermediate to those of the glycosylated and aglycosylated Fc forms.

The interparticle distance distribution functions or pairwise distributions, *P(r)* derived from the scattering curves were also compared (Figure 4b). The maximum diameter for

aglycosylated Fc was approximated at 100 Å whereas the aglycosylated Fc5 and glycosylated Fc had a maximum diameter of 95 Å. The R_g values derived from *P(r)* curves were consistent with the calculated values from the Guinier analysis (Table 3). Minor differences in between the three *P(r)* curves can be seen in the 20–35 Å regions with the aglycosylated Fc5 curve falling in between the glycosylated Fc and aglycosylated Fc.

Discussion

In this study, we describe the structure of a human, aglycosylated, *E. coli* expressed Fc domain determined by X-ray crystallography. The major structural differences between fully glycosylated Fc domains capable of binding to immune effector receptors and the aglycosylated structure presented herein are a "closing" of the C_H2 domains and disorder within the C′E loop containing N297 (the glycan attachment point on the C_H2 domain).

C′E loop flexibility has previously been reported in glycan truncated Fc structures as well as in a deglycosylated murine Fc and a human aglycosylated C_H2 domain.(14, 15, 29) The normally rigid glycosylated C′E loop is known to be crucial to certain FcγR binding interactions.(37) The lack of glycan stabilization of the C′E loop noted in our structure and others is likely at least partially responsible for the lack of effector binding in Fc domains lacking glycans. Recent crystallographic data also indicated that carbohydrates on FcγRIII can productively interact with Fc N297 carbohydrates in the absence of fucosylation(38). Fc domains lacking N297 glycosylation would lose any beneficial carbohydrate-carbohydrate interactions for FcγRIII binding as well.

In addition to changes in the C′E loop, a more closed orientation of C_H2 domains is noticeable in both aglycosylated Fc dimers present in our structure. A progressive closure of the C_H2 domains has been noted in crystal structures of Fcs with enzymatically truncated(14) and fully removed glycans.(15) This collapse of the C_H2 domains has also been suggested to be at least partially responsible for the loss of effector affinity.(15) A deglycosylated Fc structure (PDB ID: 3DNK) has also been deposited without a closed C_H2 domain. Indeed, 3DNK has a more open orientation than even some glycosyated Fc structures (Table 2). This deglycosylated, yet more open structure counters the notion that removing N297 glycans leaves a closed, collapsed Fc. Taken as a whole, the crystallographic evidence suggests that Fcs lacking glycans can adopt a number of possible orientations, and the observed orientation in crystals may be highly dependent on the crystal packing environment and therefore might not reflect the state of these molecules in solution. Interestingly, differences in the degree of "openness" between fully glycosylated Fc structures have also been noted,(32) although not nearly to the extent seen in Fc structures lacking glycans (Figure 3, Table 2). We speculate that part of the role of the N297 glycan is to limit the dynamic nature of the C_H2 domains, and restrict range of movement of the domains.

To reconcile the disparate crystallographic data on the "openness" of the aglycosylated Fc domain we chose to examine structural parameters in solution via SAXS. SAXS data indicated surprisingly that *E. coli* produced aglycosylated Fc domains actually had a larger R_g than glycosylated human Fc, thus suggesting that aglycosylated Fc domains have a more open C_H2 orientation in solution. SAXS scattering curves describe an average of the possible conformations a protein adopts in solution. The collapsed C_H2 orientations seen in X-ray structures may be one of multiple forms that Fc domains lacking glycans are able to adopt, however our SAXS data suggest that in solution they commonly adopt a conformation with a higher R_g than glycosylated Fc domains.

Interestingly, the aglycosylated Fc mutant Fc5 (E382V/M428I) had R_g 0.4 Å smaller than wildtype aglycosylated Fc (Table 3). This smaller R_g may be indicative of a structural change caused by the mutations in C_H3 that increases binding to FcγRI at the apex of the C_H2 domain. We suspected that the C_H2- C_H3 region of aglycosylated Fcs may be fertile ground for allosterically modifying distal effector functions.(19, 20)

Methods

Expression and purification of aglycosylated Fc proteins

E. coli Jude-1 (F′ [Tn*10*(Tet^r) proAB$^+$ *lacI*^{q} Δ(*lacZ*)M15] *mcrA* Δ (*mrr-hsdRMS-mcrBC*) φ80dlacZΔM15 Δ*lacX74 deoR recA1 araD139* Δ(*ara leu*)7697 *galU galK rpsL endA1 nupG*) cells harboring pTrc99A-DsbA-Fc(20) encoding either wild-type or Fc5 were cultured in 4 L flasks with 2.5 L working volume of Terrific Broth (TB) media at 37 °C. The shake flasks were transferred to 30 °C and 1 mM IPTG was added and cells (OD600 approximately 0.6) were grown overnight (14hr). The cells were then harvested and the supernatant was separated from cells by centrifugation at 9,000 rpm for 30 min. The culture supernatant was then filtered through a 0.45 μm filter. One ml of Immobilized Protein A agarose (Pierce Biotechnology) was and added to the filtered supernatant and incubated overnight at 4 °C with gentle stirring. The immobilized Protein A agarose was then collected in a column and washed with 50 ml PBS (pH 7.2). The column was then eluted using 0.1 M glycine (pH 2.7) and neutralized immediately with 1 M Tris (pH 8.0). Fc containing fractions were concentrated by ultrafiltration (10 kDa Mw cutoff) and purified by gel filtration on a Superdex G75 column (Amersham Pharmacia). Aglycosylated Fc, Fc5 and glycosylated Fc (Bethyl Laboratories) were then concentrated by ultrafiltration (10 kDa Mw cutoff) and the buffer was exchanged to 20mM Tris (pH 8) with 5% Glycerol. All Fc domains were confirmed to be dimers in solution by gel filtration.

X-ray Crystallography

Crystals of aglycosylated Fc were obtained in sitting drops using 15 mg/mL Fc added 1:1 to a mother liquor of 10% PEG 1000, 20% PEG 6000, 0.1 M magnesium chloride and 0.2 M Tris HCL, pH 7.0. Cryo-cooling in liquid nitrogen was achieved using the mother liquor plus 20% glycerol as a cryoprotectant. A 3.1 Å resolution data set was collected from at Beamline 8.3.1 at the Advanced Light Source (Lawrence Berkeley National Laboratories). Diffraction data were scaled and integrated using HKL2000.(39) Molecular replacement was successfully performed using PHASER(40, 41) with the C_H2 and C_H3 domains from PDB 3DNK as the search model. Two dimers were found in the asymmetric unit using PHASER. The model was refined using Refmac(42) in the CCP4i suite.(43) Non-crystallographic symmetry (NCS) restraints(44) were used throughout refinement with C_H2 and C_H3 domains of chains A–D linked with the exception of residues 335–345 (the region connecting C_H2 and C_H3) and the C′E loops. A and C chains and B and D chains of the C′E loop were linked by NCS due to tight crystal packing in the C′E loops of chains B and D. No electron density detected for N-terminal residues 221–235 (hinge residues) and C terminal residues 445–447; these residues are not in the models. Figures were generated with PyMOL.(45)

Small Angle X-ray Scattering

Prior to the SAXS experiments, all Fc domains were dialyzed into a 20 mM Tris (pH 8) buffer with 5% Glycerol as a cryoprotectant. SAXS data were collected at the SIBYLS beamline of the Advanced Light Source (Lawrence Berkeley National Laboratories). SAXS data were collected on 3 serial dilutions of each sample preparation at 5, 2.5 and 1.25 mg ml^{-1}. All data were collected with 1 Å X-rays. Three exposures were taken for each sample, first a short exposure (0.5 s), then a long exposures of 5 s, followed by an additional 0.5 s

exposure to check for radiation damage. The sample cell was washed between protein solutions using a mild detergent soak followed by 3 rinses with buffer solution. Data for buffer alone was also collected before and after each protein sample and subtracted from the sample curve.

The radius of gyration (R_g), which is defined as the root mean squared (rms) distance of all atoms from their common center of mass, was derived using Guinier analysis(36) in regions where $QR_g < 1.3$ using the program PRIMUS.(46, 47) Pair distribution functions were generated using the program GNOM.(48) The maximum diameter of the particle (Dmax) was adjusted in 5 Å increments in GNOM to maximize the goodness-of-fit parameter.

Acknowledgments

This work was supported by grants from the Clayton Foundation for Research and by a High Risk High Impact award from the Cancer Prevention and Research Initiative of Texas (CPRIT). We would also like to thank M. Hammel at the SIBLYS beamline for assistance in SAXS data collection. Instrumentation and technical assistance for this work were provided by the Macromolecular Crystallography Facility, with financial support from the College of Natural Sciences, the Office of the Executive Vice President and Provost, and the Institute for Cellular and Molecular Biology at the University of Texas at Austin.The Berkeley Center for Structural Biology is supported in part by the National Institutes of Health, National Institute of General Medical Sciences, and the Howard Hughes Medical Institute. The Advanced Light Source is supported by the Director, Office of Science, Office of Basic Energy Sciences, of the U.S. Department of Energy under Contract No. DE-AC02–05CH11231.

References

1. Nimmerjahn F, Ravetch J. Antibodies, Fc receptors and cancer. Curr Opin Immunol. 2007; 19:239–245. [PubMed: 17291742]
2. Nimmerjahn F, Ravetch J. Fc receptors as regulators of immune responses. Nat Rev Immunol. 2008; 8:34–47. [PubMed: 18064051]
3. Jefferis R, Lund J, Pound JD. IgG-Fc-mediated effector functions: molecular definition of interaction sites for effector ligands and the role of glycosylation. Immunol Rev. 1998; 163:59–76. [PubMed: 9700502]
4. Jefferis R. Glycoforms of human IgG in health and disease. Trends in Glycosci Glyc. 2009; 21:105–117.
5. Nesspor TC, Raju TS, Chin CN, Vafa O, Brezski RJ. Avidity confers FcgR binding and immune effector function to aglycosylated immunoglobulin G1. J Mol Recognit. 2012; 25:147–154. [PubMed: 22407978]
6. Tao MH, Morrison SL. Studies of aglycosylated chimeric mouse-human IgG - Role of carbohydrate in the structure and effector functions mediated by the human IgG constant region. J Immunol. 1989; 143:2595–2601. [PubMed: 2507634]
7. Walker MR, Lund J, Thompson KM, Jefferis R. Aglycosylation of human IgG1 and IgG3 monoclonal antibodies can eliminate recognition by human cells expressing FcgammaRI and or FcgammaRII receptors. Biochem J. 1989; 259:347–353. [PubMed: 2524188]
8. Beck A, Cochet O, Wurch T. GlycoFi's technology to control the glycosylation of recombinant therapeutic proteins. Expert Opin Drug Dis. 2010; 5:95–111.
9. Jefferis R. Glycosylation as a strategy to improve antibody-based therapeutics. Nat Rev Drug Dis. 2009; 8:226–234.
10. Niwa R, Sakurada M, Kobayashi Y, Uehara A, Matsushima K, Ueda R, Nakamura K, Shitara K. Enhanced natural killer cell binding and activation by low-fucose IgG1 antibody results in potent antibody-dependent cellular cytotoxicity induction at lower antigen density. Clin Cancer Res. 2005; 11:2327–2336. [PubMed: 15788684]
11. Okazaki A, Shoji-Hosaka E, Nakamura K, Wakitani M, Uchida K, Kakita S, Tsumoto K, Kumagai I, Shitara K. Fucose depletion from human IgG1 oligosaccharide enhances binding enthalpy and association rate between IgG1 and Fc gamma RIIIa. J Mol Biol. 2004; 336:1239–1249. [PubMed: 15037082]

12. Shields RL, Lai J, Keck R, O'Connell LY, Hong K, Meng YG, Weikert SHA, Presta LG. Lack of fucose on human IgG1 N-linked oligosaccharide improves binding to human Fc gamma RIII and antibody-dependent cellular toxicity. J Biol Chem. 2002; 277:26733–26740. [PubMed: 11986321]
13. Shinkawa T, Nakamura K, Yamane N, Shoji-Hosaka E, Kanda Y, Sakurada M, Uchida K, Anazawa H, Satoh M, Yamasaki M, Hanai N, Shitara K. The absence of fucose but not the presence of galactose or bisecting N-acetylglucosamine of human IgG1 complex-type oligosaccharides shows the critical role of enhancing antibody-dependent cellular cytotoxicity. J Biol Chem. 2003; 278:3466–3473. [PubMed: 12427744]
14. Krapp S, Mimura Y, Jefferis R, Huber R, Sondermann P. Structural analysis of human IgG-Fc glycoforms reveals a correlation between glycosylation and structural integrity. J Mol Biol. 2003; 325:979–989. [PubMed: 12527303]
15. Feige MJ, Nath S, Catharino SR, Weinfurtner D, Steinbacher S, Buchner J. Structure of the Murine Unglycosylated IgG1 Fc Fragment. J Mol Biol. 2009; 391:599–608. [PubMed: 19559712]
16. Jefferis R. Aglycosylated antibodies and the methods of making and using them: WO2008030564. Expert Opin Ther Pat. 2009; 19:101–105. [PubMed: 19441902]
17. Mazor Y, Van Blarcom T, Mabry R, Iverson B, Georgiou G. Isolation of engineered, full-length antibodies from libraries expressed in Escherichia coli. Nat Biotech. 2007; 25:563–565.
18. Simmons L, Reilly D, Klimowski L, Shantha Raju T, Meng G, Sims P, Hong K, Shields R, Damico L, Rancatore P. Expression of full-length immunoglobulins in Escherichia coli: rapid and efficient production of aglycosylated antibodies. J Immunol Methods. 2002; 263:133–147. [PubMed: 12009210]
19. Jung ST, Kang TH, Kelton W, Georgiou G. Bypassing glycosylation: engineering aglycosylated full-length IgG antibodies for human therapy. Curr Opin Biotech. 2011; 22:858–67. [PubMed: 21420850]
20. Jung ST, Reddy ST, Kang TH, Borrok MJ, Sandlie I, Tucker PW, Georgiou G. Aglycosylated IgG variants expressed in bacteria that selectively bind Fc gamma RI potentiate tumor cell killing by monocyte-dendritic cells. Proc Natl Acad Sci U S A. 2010; 107:604–609. [PubMed: 20080725]
21. Sazinsky SL, Ott RG, Silver NW, Tidor B, Ravetch JV, Wittrup KD. Aglycosylated immunoglobulin G1 variants productively engage activating Fc receptors. Proc Natl Acad Sci U S A. 2008; 105:20167–20172. [PubMed: 19074274]
22. Lu JH, Ellsworth JL, Hamacher N, Oak SW, Sun PD. Crystal Structure of Fc gamma Receptor I and Its Implication in High Affinity gamma-Immunoglobulin Binding. J Biol Chem. 2011; 286:40608–40613. [PubMed: 21965667]
23. Shields RL, Namenuk AK, Hong K, Meng YG, Rae J, Briggs J, Xie D, Lai J, Stadlen A, Li B, Fox JA, Presta LG. High resolution mapping of the binding site on human IgG1 for Fc gamma RI, Fc gamma RII, Fc gamma RIII, and FcRn and design of IgG1 variants with improved binding to the Fc gamma R. J Biol Chem. 2001; 276:6591–6604. [PubMed: 11096108]
24. Radaev S, Sun P. Recognition of immunoglobulins by Fc gamma receptors. Mol Immunol. 2002; 38:1073–1083. [PubMed: 11955599]
25. Matsumiya S, Yamaguchi Y, Saito J, Nagano M, Sasakawa H, Otaki S, Satoh M, Shitara K, Kato K. Structural comparison of fucosylated and nonfucosylated Fc fragments of human immunoglobulin G1. J Mol Biol. 2007; 368:767–779. [PubMed: 17368483]
26. Mimura Y, Church S, Ghirlando R, Ashton PR, Dong S, Goodall M, Lund J, Jefferis R. The influence of glycosylation on the thermal stability and effector function expression of human IgG1-Fc: properties of a series of truncated glycoforms. Mol Immunol. 2000; 37:697–706. [PubMed: 11275255]
27. Mimura Y, Sondermann P, Ghirlando R, Lund J, Young SP, Goodall M, Jefferis R. Role of oligosaccharide residues of IgG1-Fc in Fc gamma RIIb binding. J Biol Chem. 2001; 276:45539–45547. [PubMed: 11567028]
28. Matsumiya S, Yamaguchi Y, Saito J, Nagano M, Sasakawa H, Otaki S, Satoh M, Shitara K, Kato K. Corrigendum to "Structural Comparison of Fucosylated and Nonfucosylated Fc Fragments of Human Immunoglobulin G1" (vol 386, pg 767, 2007). J Mol Biol. 2011; 408:1001–1001.

29. Prabakaran P, Vu BK, Gan JH, Feng Y, Dimitrov DS, Ji XH. Structure of an isolated unglycosylated antibody C(H)2 domain. Acta Crystallogr D. 2008; 64:1062–1067. [PubMed: 18931413]
30. Kato K, Sautes-Fridman C, Yamada W, Kobayashi K, Uchiyama S, Kim H, Enokizono J, Galinha A, Kobayashi Y, Fridman WH, Arata Y, Shimada I. Structural basis of the interaction between IgG and Fc gamma receptors. J Mol Biol. 2000; 295:213–224. [PubMed: 10623521]
31. Frauenfelder H, Petsko GA, Tsernoglou D. Temperature-dependent X-ray diffraction as a probe of protein structural dynamics. Nature. 1979; 280:558–563. [PubMed: 460437]
32. Oganesyan V, Damschroder MM, Leach W, Wu H, Dall'Acqua WF. Structural characterization of a mutated, ADCC-enhanced human Fc fragment. Mol Immunol. 2008; 45:1872–1882. [PubMed: 18078997]
33. Borrok MJ, Zhu YM, Forest KT, Kiessling LL. Structure-Based Design of a Periplasmic Binding Protein Antagonist that Prevents Domain Closure. ACS Chem Biol. 2009; 4:447–456. [PubMed: 19348466]
34. Komeiji Y, Ueno Y, Uebayasi M. Molecular dynamics simulations revealed Ca2+-dependent conformational change of calmodulin. FEBS lett. 2002; 521:133–139. [PubMed: 12067741]
35. Shilton B, Flocco M, Nilsson M, Mowbray S. Conformational changes of three periplasmic receptors for bacterial chemotaxis and transport: the maltose-, glucose/galactose-and ribose-binding proteins. J Mol Biol. 1996; 264:350–363. [PubMed: 8951381]
36. Guinier, A.; Fournet, G., editors. Small-Angle Scattering of X-rays. John Wiley and Sons; New York: 1955.
37. Sondermann P, Huber R, Oosthuizen V, Jacob U. The 3.2-angstrom crystal structure of the human IgG1 Fc fragment-Fc gamma RIII complex. Nature. 2000; 406:267–273. [PubMed: 10917521]
38. Ferrara C, Grau S, Jager C, Sondermann P, Brunker P, Waldhauer I, Hennig M, Ruf A, Rufer AC, Stihle M, Umana P, Benz J. Unique carbohydrate-carbohydrate interactions are required for high affinity binding between Fc gamma RIII and antibodies lacking core fucose. Proc Natl Acad Sci U S A. 2011; 108:12669–12674. [PubMed: 21768335]
39. Otwinowski Z, Minor W. Processing of X-ray diffraction data collected in oscillation mode. Methods Enzymol. 1997; 276:307–326.
40. McCoy A, Grosse-Kunstleve R, Storoni L, Read R. Likelihood-enhanced fast translation functions. Acta Crystallogr D. 2005; 61:458–464. [PubMed: 15805601]
41. Storoni L, McCoy A, Read R. Likelihood-enhanced fast rotation functions. Acta Crystallogr D. 2004; 60:432–438. [PubMed: 14993666]
42. Winn M, Murshudov G, Papiz M. Macromolecular TLS refinement in REFMAC at moderate resolutions. Method Enzymol. 2003; 374:300–321.
43. Winn M. An overview of the CCP4 project in protein crystallography: an example of a collaborative project. Journal of synchrotron radiation. 2002; 10:23–25. [PubMed: 12511787]
44. Kleywegt G. Use of non-crystallographic symmetry in protein structure refinement. Acta Crystallogr D. 1996; 52:842–857. [PubMed: 15299650]
45. DeLano, W. The PyMOL molecular graphics system. DeLano Scientific; Palo Alto, CA, USA: 2002. http://www.pymol.org
46. Konarev P, Petoukhov M, Volkov V, Svergun D. ATSAS 2.1, a program package for small-angle scattering data analysis. JAppl Crystallogr. 2006; 39:277–286.
47. Konarev P, Volkov V, Sokolova A, Koch M, Svergun D. PRIMUS: a Windows PC-based system for small-angle scattering data analysis. J Appl Crystallogr. 2003; 36:1277–1282.
48. Svergun DI. Restoring low resolution structure of biological macromolecules from solution scattering using simulated annealing. Biophys J. 1999; 76:2879–2886. [PubMed: 10354416]
49. Deisenhofer J. Crystallographic refinement and atomic models of a human Fc Fragment and its complex with fragment-B of Protein-A from Staphylococcus aureus at 2.9 Å and 2.8 Å resolution. Biochem. 1981; 20:2361–2370. [PubMed: 7236608]
50. Saphire EO, Parren P, Pantophlet R, Zwick MB, Morris GM, Rudd PM, Dwek RA, Stanfield RL, Burton DR, Wilson IA. Crystal structure of a neutralizing human IgG against HIV-1: A template for vaccine design. Science. 2001; 293:1155–1159. [PubMed: 11498595]

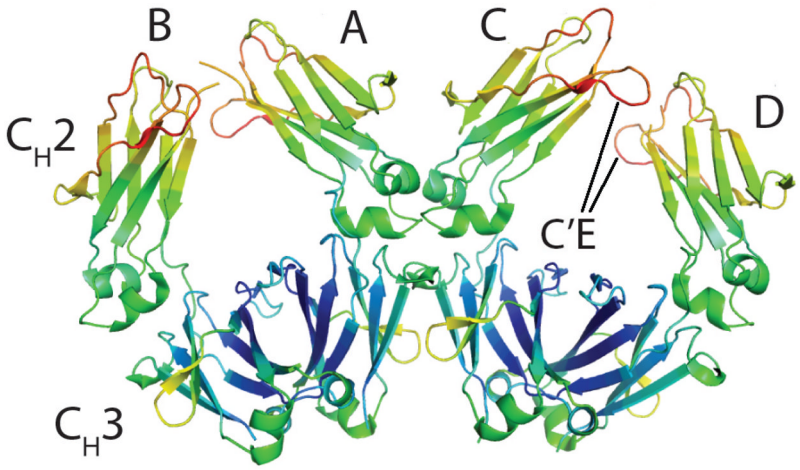

Figure 1.

Overall structure of aglycosylated IgG Fc domain solved at 3.1 Å resolution. The range of *B*-factors of all Cαs are represented by rainbow-colors ranging from blue (low) to red (high). Two homodimers A,B and C,D are present in the asymmetric unit. The location of the C′E loop is noted in the C,D dimer.

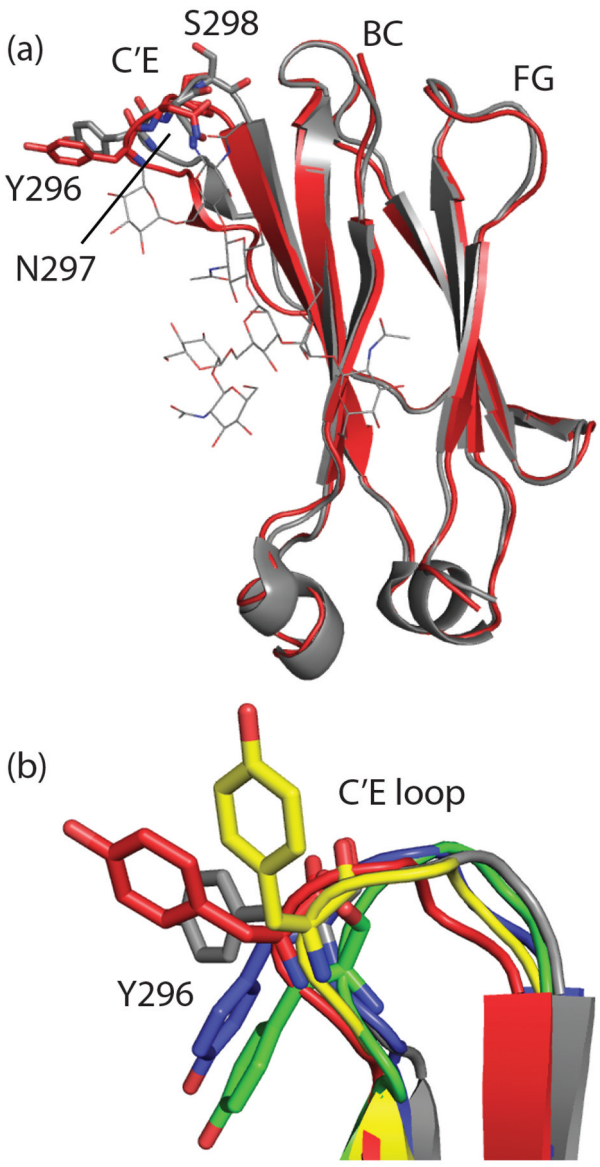

Figure 2.

Comparison of C′E loops of glycosylated and aglycosylated C_H2 domains. (a) The A chain C_H2 domain of the glycosylated Fc 3AVE (grey) is aligned with the A chain of our aglycosylated C_H2 domain (3S7G, red). Differences in the C′E loop orientation can be seen in the ribbon diagram. Y296, N297 and S298 orientations at the apex of the C′E loop differ significantly between glycosylated and aglycosylated C_H2 domains. (b) The C′E loops of glycosylated 3AVE (grey) are shown aligned with three previously solved C_H2 domains lacking glycosylation, 2DJ9 (yellow), 3DNK (blue), 3S7G A chain (red) and 3S7G B chain (green). Y296 side chain orientations differ significantly from the glycosylated structure and each other.

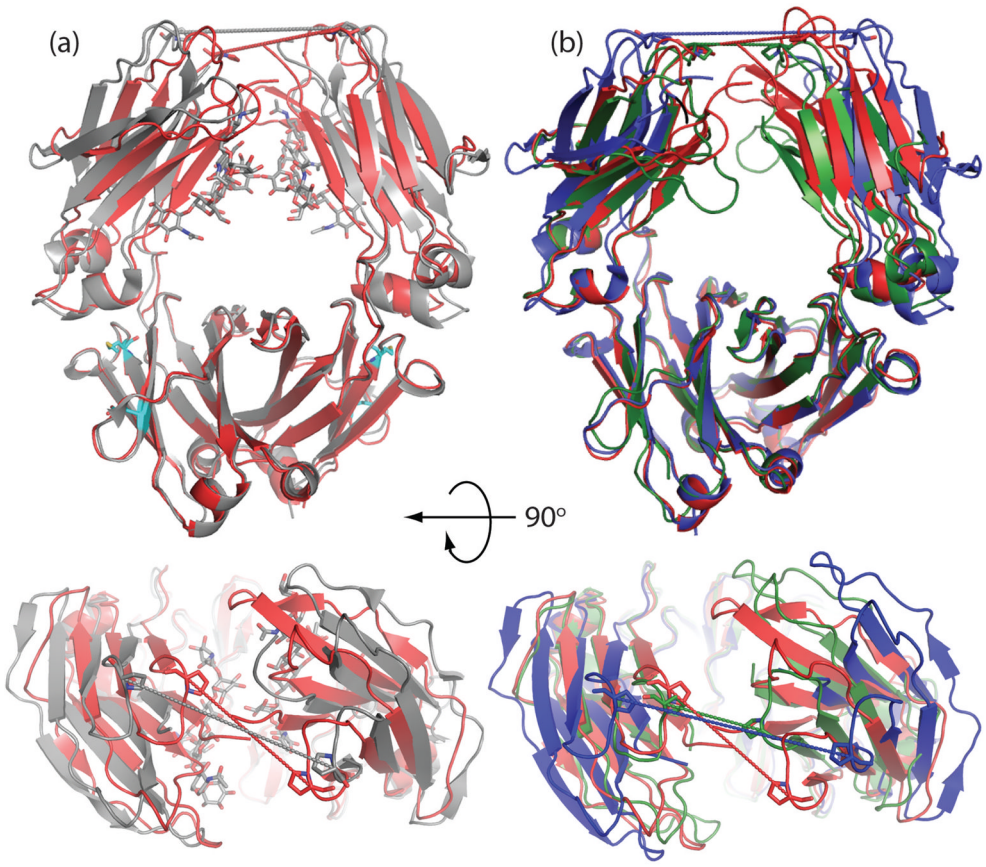

Figure 3.

Comparison of overall opening/closing of C_H2 domains among glycosylated and deglycosylated structures. (a) Glycosylated Fc 3AVE (grey) is compared with the A,B dimer of aglycosylated 3S7G (red). Pro 329 distances (measured from Cαs) are shown as dotted lines. P329 distances for 3AVE and 3S7G are 25.1 Å and 18.5 Å respectively. E382 and M428 are represented as sticks (cyan) to highlight the location of the Fc5 mutation (b) The A,B dimer of aglycosylated 3S7G (red) is compared with deglycosylated human Fc, 3DNK (blue) and the deglycosylated mouse Fc, 3HKF (green). P329 distances for 3DNK and 3HKF are 27.6 Å and 11.6 Å respectively.

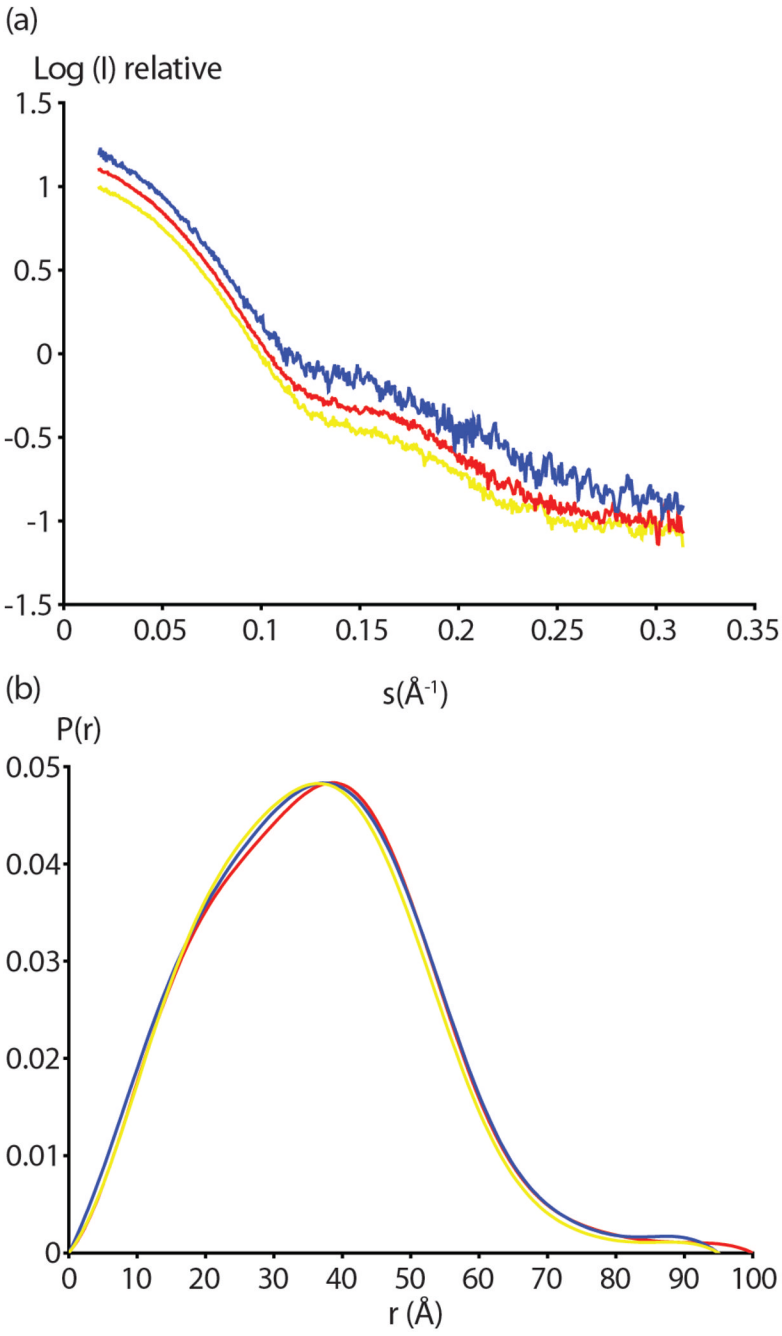

Figure 4.

SAXS analysis of glycosylated and aglycosylated Fcs. (a) Scattering profiles from 0.5 second exposure are shown for glycosylated Fc (yellow) aglycosylated Fc (red) and aglycosylated Fc5 (blue). These profiles were obtained by extrapolating curves at different concentrations to the zero concentration. The logarithm of scattering intensity is shown as a function of the reciprocal vector (S). (b) The distance distribution functions (*P(r)*) of glycosylated Fc (yellow) aglcyosylated Fc (red) and aglycosylated Fc5 (blue) are shown. Curves were calculated from the SAXS scattering data in (a).

Table 1

Data collection and refinement statistics

Data collection	
Space group	P1
Cell dimensions	
a, b, c (Å)	98.2, 100.5, 116.9
α, β, γ (°)	65.7, 65.8, 77.8
Resolution (Å)	50–3.13 (3.26-3.13)[a]
Rsym (%)	6.1 (34.7) [a]
I/σI	12.6 (2.8) [a]
Completeness (%)	98.2 (97.1) [a]
Redundancy	1.9 (1.9) [a]
Refinement	
Resolution (Å)	45–3.13 (3.24-3.13) [a]
No. reflections	17958 (925) [a]
Rcryst/Rfree (%)	26.2/32.3 (35.1/38.3) [a]
No. atoms	
Protein	6640
Water	22
Wilson B-factor	87.2
R.m.s. deviations	
Bond lengths (Å)	0.014
Bond angles (°)	1.46
PDB code	3S7G

[a]Values in parentheses correspond to the highest resolution shell.

Table 2

Proline 329 distances for Fc structures with and without N297 Glycans. Structures lacking the N297 glycan are in Italics

PDB ID	Chains	Space Group	Resolution (Å)	P329 Distance (Å)	Reference
3S7G	A,B	P1	3.1	18.9	This Study
3S7G	C,D	P1	3.1	19.6	This Study
3DNK	A,B	$P2_12_12_1$	2.8	27.6	Unpublished
3HKF	A	$P6_122$	2.5	11.6*	(15)
3AVE	A,B	$P2_12_12_1$	2.0	25.1	(25, 28)
2DTS	A,B	$P2_12_12_1$	2.2	24.2	(25)
1H3Y	A,B	$P6_122$	4.1	29.6	(14)
1H3W	M	$C222_1$	2.85	33.8	(14)
1H3X	A,B	$P2_12_12_1$	2.4	22.6	(14)
1H3V	A,B	$P2_12_12_1$	2,4	26.9	(14)
1FC1	A,B	$P2_12_12_1$	2.9	26.8	(49)
1HZH	A,B	H32	2.7	23.5	(50)

*For the murine Fc (2HKF) Pro332 distances are measured.

Table 3

Observed R_g values for aglycosylated and glycosylated Fcs (in Å)

	R_g Guinier (0.5s exposure)	**R_g Guinier (5s exposure)**	**R_g *P(r)***
aglycosylated Fc (wt)	**28.3±0.1**	28.4±0.1	28.2±0.1
aglycosylated Fc5	**27.9±0.1**	28.0±0.2	28.0±0.1
glycosylated Fc (wt)	**27.4±0.1**	27.2±0.1	27.5±0.1